Validation of the linear ideal magnetohydrodynamic model of three-dimensional tokamak equilibria

M. J. Lanctot,[1,a)] H. Reimerdes,[1] A. M. Garofalo,[2] M. S. Chu,[2] Y. Q. Liu,[3] E. J. Strait,[2] G. L. Jackson,[2] R. J. La Haye,[2] M. Okabayashi,[4] T. H. Osborne,[2] and M. J. Schaffer[2]

[1]*Columbia University, 2960 Broadway, New York, New York 10027-1754, USA*
[2]*General Atomics, P.O. Box 85608, San Diego, California 92186-5608, USA*
[3]*EURATOM/CCFE Fusion Association, Abingdon, Oxon OX143DB, United Kingdom*
[4]*Princeton Plasma Physics Laboratory, P.O. Box 451, Princeton, New Jersey 08543-0451, USA*

The first quantitative comparison of linear ideal magnetohydrodynamic (MHD) theory with external magnetic measurements of the nonaxisymmetric plasma perturbation driven by external long-wavelength magnetic fields in high-temperature tokamak plasmas is presented. The comparison yields good (within 20%) agreement for plasma pressures up to ~75% of the ideal stability limit calculated without a conducting wall. For higher plasma pressures, the ideal MHD model tends to overestimate the perturbed field indicating the increasing importance of stabilizing nonideal effects. © *2010 American Institute of Physics.* [doi:10.1063/1.3335237]

In the ideal tokamak, magnetic surfaces are axisymmetric in the toroidal dimension. Until recently, small deviations from axisymmetry ($\delta B/B_T \sim 10^{-4}$) were associated with adverse effects such as reduced plasma confinement and plasma-terminating instabilities. These effects are linked to the formation of magnetic islands that are driven by so called pitch-resonant magnetic fields. The resonance occurs on flux surfaces where the safety factor is a rational number when nonaxisymmetric currents outside the plasma drive a magnetic perturbation normal to the surface (δB_r^{ext}) with a structure that matches the helicity of the unperturbed magnetic field line. [The safety factor (q) is the ratio of the average number of toroidal circuits to the average number of poloidal circuits made by a magnetic field line.] A decomposition of δB_r^{ext} using helical harmonics with m poloidal and n toroidal periods in a straight field line coordinate system allows the resonant components to be identified by the criterion, $m = qn$.[1] Contrary to previous conceptions, a paradigm is emerging in which nonaxisymmetric fields are associated with improved plasma performance. For example, resonant magnetic perturbations can be used to suppress edge localized modes (ELMs),[2] instabilities that result in potentially damaging heat pulses to the tokamak divertor. In addition, nonaxisymmetric fields with dominantly nonresonant components have been found to drive significant plasma rotation,[3] which is known to be favorable for stability.

When considering three-dimensional field effects, it is important to account for the plasma response (δB^{plas}), which is the magnetic field resulting from perturbed currents in the plasma.[4] Observations in marginally stable discharges[5,6] and in plasmas far from a stability limit[7] indicate that the δB^{plas} significantly alters the total perturbed field, δB. In the Joint European Torus (JET),[8] the plasma response is known to depend strongly on the plasma β particularly near the no-wall limit, which is the stability limit calculated without a conducting wall surrounding the plasma.[9,10] Here

$\beta = 2\mu_0 \langle p \rangle / B_0^2$, where $\langle p \rangle$ is the volume-averaged plasma pressure, μ_0 is the magnetic permeability, and B_0 is the magnetic field at the magnetic axis. An increased sensitivity to external fields at high-pressure results because the energy required to drive a kinklike perturbation in the plasma vanishes near the stability limit.[4] In DIII-D,[11] this β dependence leads to a decrease in the observed tolerance to external $n=1$ magnetic fields,[12] and to amplified torque from nonresonant fields in high-β plasmas.[3] It is reasonable to postulate that δB^{plas} also plays a role in ELM suppression since the plasma response modifies both resonant and nonresonant components of applied magnetic perturbations. Progress in the aforementioned areas depends in part on the development of validated plasma response models that can quantify the dependence of δB^{plas} on plasma parameters, and inform the design of future machines such as ITER.[13]

In this letter, we present the first quantitative comparison of linear ideal magnetohydrodynamic (MHD) theory with external magnetic measurements of the nonaxisymmetric plasma perturbation driven by applied $n=1$ magnetic fields. The results identify the conditions in which ideal MHD alone can describe δB^{plas}, and where nonideal effects on the plasma stability become important.

Measurements of nonaxisymmetric equilibria in DIII-D are obtained by probing high-temperature tokamak plasmas with external $n=1$ magnetic fields. Neutral beam injection (NBI) is used to heat a high confinement mode (H-mode) diverted discharge with an upper triangularity of 0.12, Fig. 1(a). In discharge 135773, the normalized plasma β, $\beta_N = \beta/(I_p/aB_0)$, is maintained near 2.0% mT/MA using feedback control of the NBI, Fig. 2(a). Here I_p is the plasma current and a is the plasma minor radius. To maximize the toroidal plasma rotation, Fig. 2(b), only NBI heating in the plasma current direction (co-NBI) is used. This results in a greater resilience to error field driven rotation collapses and locked modes, and permits well-resolved plasma response measurements to be made over a wide range of β_N and applied field magnitudes. The equilibrium pressure and current
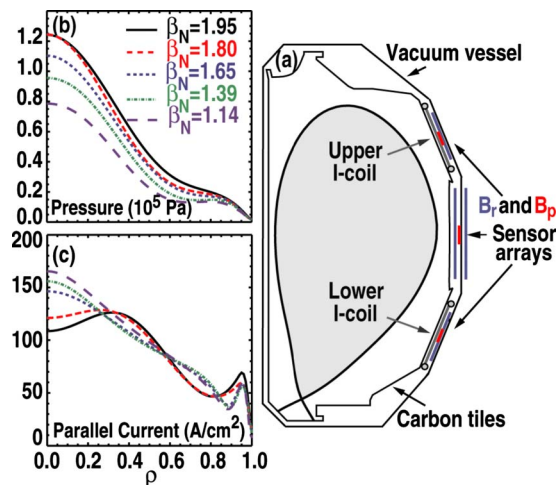
FIG. 1. (Color online) (a) Schematic showing the I-coil, magnetic sensors, plasma separatrix, and the vacuum vessel. Radial and poloidal field probes are located at, above, and below the midplane. (b) Plasma pressure and (c) parallel current density profiles in discharges 135 762, 135761, 135758, 135765, and 135773 at 1805 ms in which the normalized beta was varied from 1.14 to 1.95 mT/MA.

profiles discussed here are shown in Figs. 1(b) and 1(c) as a function of the flux coordinate $\rho=\sqrt{\psi_t}$, where ψ_t is the toroidal flux. A rotating $n=1$ magnetic perturbation is applied, Fig. 2(c), together with empirically determined error field correction currents using the internal coil on DIII-D (I-coil), a set of 12 single-turn magnetic field coils located inside the vacuum vessel above and below the midplane, Fig. 1(a). A field rotation frequency of 10 Hz is chosen to use synchronous detection of the plasma response while avoiding attenuation of the external field due to eddy currents in the vacuum vessel. By varying the toroidal phase difference ($\Delta\phi$) between currents in the upper and lower I-coil arrays, the sen-
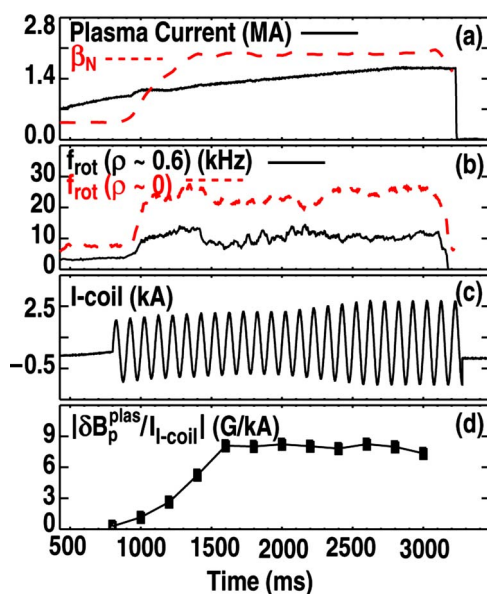

FIG. 2. (Color online) (a) Time evolution of the plasma current (solid), the plasma beta (dashed), (b) the core (dashed) toroidal carbon VI rotation, the rotation at $\rho=0.6$ (solid), (c) the current in one segment of the I-coil, and (d) the normalized perturbed poloidal field at the midplane due to the plasma, $\delta B_p^{plas}/I_c$.

sitivity of δB^{plas} to the helical structure of δB^{ext} can be explored. The magnitudes of the resonant components of δB_r^{ext} applied with the I-coil depend on $\Delta\phi$, and are less than 1.5 G/kA of current in the I-coil. The magnitude of the perturbed poloidal field at the midplane due solely to the plasma and normalized to the applied I-coil current, $\delta B_p^{plas}/I_c$, exhibits a strong dependence on β_N, Fig. 2(d), and can exceed δB_r^{ext} by more than a factor of 10 above the no-wall limit.

The quantitative dependence of the plasma response on β_N is investigated by applying fields with $\Delta\phi=240°$ to discharges where β_N is held constant between 1.1 and 2.6% mT/MA, a range that includes the computed no-wall limit, $\beta_N^{NW}\sim2.15$. The magnetic measurements were obtained in discharges free from rotating $n=1$ tearing modes. For each discharge, internal current and kinetic profile measurements are used as input to the equilibrium fitting code EFIT to reconstruct the axisymmetric magnetic field.[14] The magnetic field pitch angle is constrained using measurements from multiple motional Stark effect (MSE) polarimeters. Since a non-negligible radial electric field is present in these discharges due to the strong toroidal plasma rotation, both the safety factor and the electric field profiles must be solved for simultaneously using MSE polarimeters that view the neutral beams from different angles.[15] The edge current profile is further constrained by calculating the bootstrap current based on the Sauter model,[16] which was shown to be accurate to within ±13% on DIII-D.[17] The calculation requires internal measurements of the experimental profiles that compose the total plasma pressure, including the fast ion pressure obtained from a transport calculation using the ONETWO code.[18]

In these discharges, the toroidal rotation profile is peaked with a core rotation frequency (ω_ϕ) of 2%–6% of the Alfvén frequency (ω_A). Although only co-NBI is used for heating, the toroidal plasma rotation did not increase significantly with the plasma beta above $\beta_N\sim1.7$ due to the braking torque from the applied nonaxisymmetric field, which was not varied systematically. Since the dynamic pressure ($P_d=\rho R^2\omega_\phi^2/2$) is only 3%–5% of the total plasma pressure, it was not considered during the equilibrium reconstructions as it has been shown to have a negligible effect on the reconstructed pressure and safety factor profiles.[14] This is in contrast to high-pressure equilibria in the National Spherical Torus Experiment (NSTX),[19] where ω_ϕ/ω_A can be an order of magnitude larger than in DIII-D, and the dynamic pressure can be as much as 25%.[20]

The MARS-F stability code is used to calculate the plasma response by solving the linear single fluid MHD equations together with equations for the vacuum magnetic field, a thin-shell approximation of a resistive axisymmetric wall, and external currents in control coils.[21] Given a toroidally axisymmetric equilibrium satisfying force balance, the equations are solved for stable, driven, helical perturbations to the plasma pressure, current, fluid displacement, and magnetic field. The MARS-F code includes models that describe the damping of resistive wall modes (RWMs). By invoking strong damping of the RWM, good agreement between plasma response calculations and magnetic measurements of the magnitude of the perturbed radial field at the midplane has been found in the JET.[10] However, in this study, the
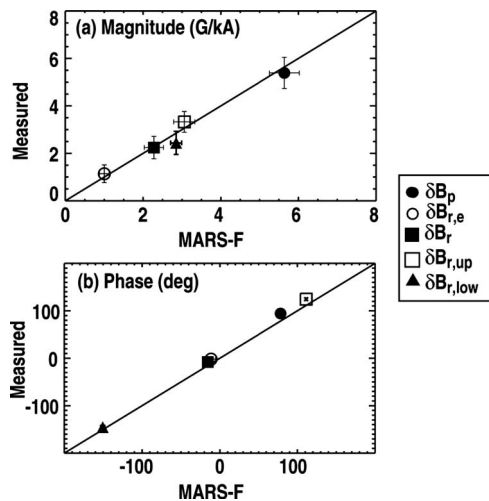
FIG. 3. (a) Magnitude and (b) toroidal phase of δB^{plas} at $\beta_N = 1.7$ from various magnetic diagnostics. Subscripts on δB refer to poloidal (p), or radial (r) field probes, the probe location either internal (no label) or external (e) to the vacuum vessel, and the probe elevation either at (no label), above (up) or below (low) the midplane. Solid lines mark perfect agreement between measured and modeled data. The error bars for the calculated quantities are based on a variation of the total poloidal flux between 99.0% and 99.7% of the experimentally determined flux.
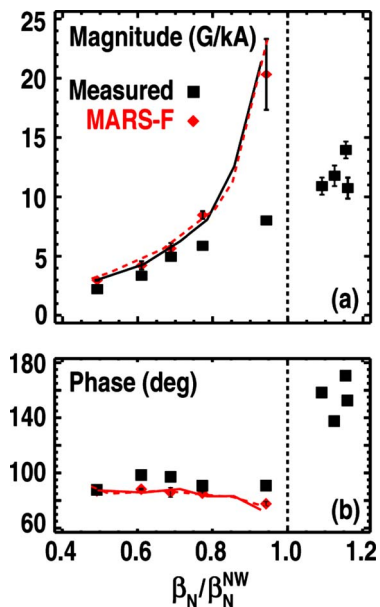

FIG. 4. (Color online) Comparison of the measured (square) and computed (diamond) (a) magnitude and (b) toroidal phase of δB_p^{plas} at the midplane as a function of β_N / β_N^{NW}. Solid and dashed lines mark the computed δB_p^{plas} for scaled equilibria based on discharges with $\beta_N = 1.14$ and $\beta_N = 1.95$.

plasma perturbation is modeled using only ideal MHD, which does not provide any free parameters that directly affect the amplitude of the plasma response. Since the influence of the background plasma rotation on the RWM stability is neglected, we focus here only on equilibria that are below the no-wall limit. This is reasonable since above the stability threshold, ideal MHD predicts an unstable RWM, which is not experimentally observed in these discharges.

Since the MARS-F code solves for the plasma response based on fixed boundary equilibria, multiple equilibria were computed for each experimental reconstruction by retaining between 99.0 and 99.7% of the total poloidal flux. These equilibria were used as input to MARS-F to calculate the plasma perturbation, and to estimate the error introduced by the flux truncation. At $\beta_N = 1.7$, both the magnitude and toroidal phase of the computed $n = 1$ perturbed field at various sensor locations are in good agreement (within 20%) with the measured plasma response, Fig. 3, which is obtained by subtracting the measured coil-sensor coupling from the total perturbed field. The measured toroidal phase is quoted with respect to the applied radial field at the midplane, and shows that δB_r^{plas} is in phase with the applied field, while δB_p^{plas} is shifted by +90° in the direction of the plasma current. The phases of the upper and lower radial magnetic probes indicate the helical structure of the perturbation. A systematic phase shift of the measurements with respect to the predictions in the direction of the plasma rotation is likely caused by the interaction of the mode with the plasma rotation. These magnetic measurements show that ideal MHD is adequate to describe the external plasma response for values of β_N sufficiently far from β_N^{NW}.

At higher pressures, MARS-F tends to overestimate the perturbed field. In Fig. 4, the measured and modeled magnitude and phase of δB_p^{plas} are compared as a function of β_N / β_N^{NW}, where β_N^{NW} is calculated for each equilibrium. In

the range of 75%–100% of β_N^{NW}, the computed δB_p^{plas} exceeds the observed magnitude by a factor of 1.5–3, and the phase shifts in the negative I_p direction. The poor agreement here indicates that nonideal effects are important even in this regime. Above β_N^{NW}, the observed phase of δB_p^{plas} shifts in the direction of I_p by 50° at $\beta_N = 2.3$, which is inconsistent with ideal MHD theory. Although there is an apparent jump in the observed phase near the no-wall limit for this data set, a larger database of plasma response measurements shows a smooth transition through the stability threshold.

The magnitude of the computed δB^{plas} depends on the stability of the plasma, which is determined in part by the details of the current profile. This is demonstrated using equilibria obtained by solving the Grad–Shafranov equation independent of the experimental constraints using a scalar multiplier to vary the pressure profile determined with EFIT while keeping the current profile fixed for the lowest and highest beta equilibria shown in Fig. 1(b). The solid and dashed lines in Fig. 4 mark the computed δB_p^{plas} based on the low and high beta discharge, which have a plasma internal inductance of 0.85 and 0.79, respectively. For all values of β_N, the computed δB_p^{plas} is larger for the plasma with a lower internal inductance. However, the δB_p^{plas} for both sets of discharges are equal when considered as a function of β_N / β_N^{NW}. This indicates that the current profile influences the plasma response, but only insofar as it affects the stability limit, which is proportional to the internal inductance.[22] However, the discrepancy between the measurements and the MHD calculations near the no-wall limit cannot be explained by a variation of the experimentally determined current profile within the known uncertainties of the bootstrap current calculation.

The plasma response also depends on the safety factor profile and the structure of δB^{ext} through a resonance with the unstable kink eigenmode, which has no pitch resonant
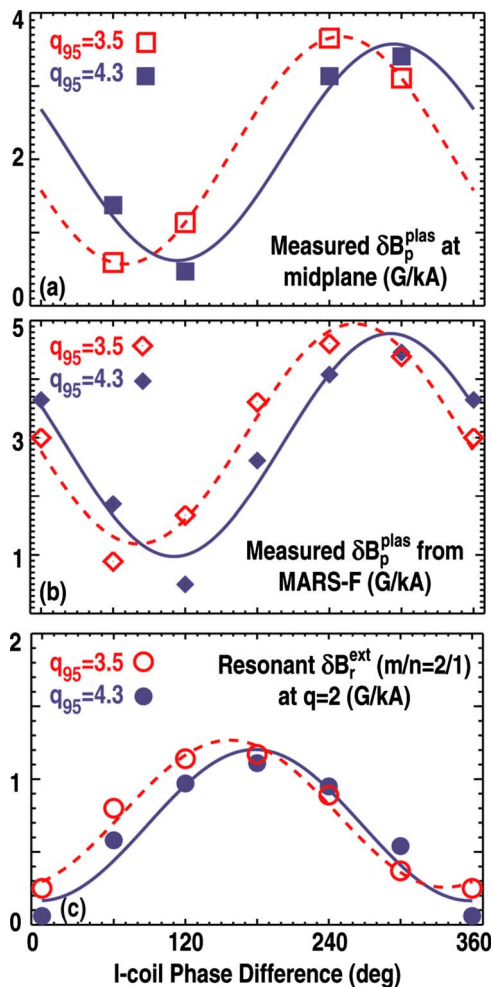
FIG. 5. (Color online) Comparison of (a) measured and (b) modeled δB_p^{plas}, and (c) the resonant $m/n=2/1$ component of δB_r^{ext} at the $q=2$ surface for two values of q_{95} as a function of $\Delta\phi$.

structure at the outboard midplane where the plasma interacts most with the external field.[12] This is demonstrated by varying $\Delta\phi$ between discharges while keeping $\beta_N=1.6$, and ramping the plasma current from 1.0 to 1.7 MA. This leads to a decrease in the safety factor profile during the discharge, which is characterized by a change in the safety factor at 95% of the poloidal flux, q_{95}. The measured δB_p^{plas} are shown in Fig. 5(a) for four values of $\Delta\phi$ at the times when q_{95} varies from 4.3 to 3.5. The maximum (minimum) plasma response for $q_{95}=4.3$ occurs for $\Delta\phi=300°$ (120°) while for $q_{95}=3.5$, the maximum (minimum) occurs at $\Delta\phi=240°$ (60°). MARS-F modeling of the $\Delta\phi$ and q_{95} dependence using two representative equilibrium reconstructions from discharge #135817 in which $\Delta\phi=60°$ qualitatively recreates the observed dependencies, Fig. 5(b). The measured and modeled plasma response trends are uncorrelated with the change in the $(m,n)=(2,1)$ resonant component of δB^{ext} at the $q=2$ surface as calculated with SURFMN, Fig. 5(c); the maximum (2,1) magnitude is applied with $\Delta\phi=180°$ and decreases with increasing $\Delta\phi$ while the plasma response is increasing. Modeling of the unstable kink eigenmode with MARS-F for both values of q_{95} reveals that the peak plasma response occurs when δB_r^{ext} is aligned with the unstable kink

structure at the location of the I-coil. An unstable mode was not observed in these discharges so the calculations were based on equilibrium reconstructions in which the pressure profile was scaled while keeping the safety factor fixed in order to obtain an unstable equilibrium.

In conclusion, measurements of the external plasma response to applied $n=1$ magnetic perturbations made in rotating, H-mode discharges on the DIII-D tokamak show the ideal MHD plasma response calculated with the MARS-F code is adequate to describe the plasma response for values of the normalized beta up to approximately 75% of the no-wall stability limit. However, ideal MHD overestimates the perturbation as the plasma approaches and exceeds the $n=1$ no-wall stability limit, highlighting the need for a nonideal theory near marginal stability. Experiments varying the pitch angle of the externally applied field at different values of plasma current demonstrate that the plasma response depends primarily on a resonance between the external field and the unstable kink eigenmode.

[1] M. J. Schaffer, J. E. Menard, M. P. Aldan *et al.*, Nucl. Fusion **48**, 024004 (2008).
[2] T. E. Evans, R. A. Moyer, K. H. Burrell *et al.*, Nat. Phys. **2**, 419 (2006).
[3] A. M. Garofalo, W. M. Solomon, M. J. Lanctot *et al.*, Phys. Plasmas **16**, 056119 (2009).
[4] A. H. Boozer, Phys. Rev. Lett. **86**, 5059 (2001).
[5] A. M. Garofalo, T. H. Jensen, and E. J. Strait, Phys. Plasmas **10**, 4776 (2003).
[6] H. Reimerdes, T. C. Hender, S. A. Sabbagh *et al.*, Phys. Plasmas **13**, 056107 (2006).
[7] J.-K. Park, M. J. Schaffer, J. E. Menard, and A. H. Boozer, Phys. Rev. Lett. **99**, 195003 (2007).
[8] P. H. Rebut, R. J. Bickerton, and B. E. Keen, Nucl. Fusion **25**, 1011 (1985).
[9] M. P. Gryaznevich, T. C. Hender, D. F. Howell *et al.*, Plasma Phys. Controlled Fusion **50**,124030 (2008).
[10] T. Hender, M. Gryaznevich, Y. Liu *et al.*, Proceedings of the 20th International Conference on Plasma Physics and Controlled Nuclear Fusion Research, Vilamoura, Portugal 2004 (unpublished).
[11] J. L. Luxon, T. C. Simonen, R. D. Stambaugh, and the DIII-D Team, Fusion Sci. Technol. **48**, 828 (2005).
[12] H. Reimerdes, A. M. Garofalo, E. J. Strait *et al.*, Nucl. Fusion **49**, 115001 (2009).
[13] M. Shimada, D. J. Campbell, V. Mukhovatov *et al.*, Nucl. Fusion **47**, S1 (2007).
[14] L. L. Lao, H. E. St. John, Q. Peng *et al.*, Fusion Sci. Technol. **48**, 968 (2005).
[15] C. T. Holcomb, M. Makowski, S. Allen, W. Meyer, and M. Van Zeeland, Rev. Sci. Instrum. **79**, 10F518 (2008).
[16] O. Sauter, C. Angioni, and Y. R. Lin-Liu, Phys. Plasmas **6**, 2834 (1999).
[17] M. R. Wade, M. Murakami, and P. A. Politzer, Phys. Rev. Lett. **92**, 235005 (2004).
[18] H. E. St. John, J. R. Ferron, L. L. Lao, T. H. Osborne, S. J. Thompson, and D. Wroblewski, *Proceedings of the 15th International Conference on Plasma Physics and Controlled Nuclear Fusion Research*, Seville, 1994 (IAEA, Vienna, 1995), Vol. 3, p. 603.
[19] M. Ono, S. Kaye, M. Peng *et al.*, Nuclear Fusion **40**, 557 (2000).
[20] S. A. Sabbagh, A. C. Sontag, J. M. Bialek *et al.*, Nucl. Fusion **46**, 635 (2006).
[21] Y. Q. Liu, A. Bondeson, C. Fransson, B. Lennartson, and C. Breitholtz, Phys. Plasmas **7**, 3681 (2000).
[22] E. J. Strait, Fusion Sci. Technol. **48**, 864 (2005).